tvst

Article

Photo-Mediated Ultrasound Therapy for the Treatment of Corneal Neovascularization in Rabbit Eyes

Yu Qin[1,2,*], Yixin Yu[3,4,7,*], Julia Fu[3], Xinyi Xie[5], Tao Wang[2], Maria A. Woodward[3], Yannis M. Paulus[2,3], Xinmai Yang[6], and Xueding Wang[2]

[1] Institute of Acoustics, School of Physics Science and Engineering, Tongji University, Shanghai, China
[2] Department of Biomedical Engineering, University of Michigan, Ann Arbor, MI, USA
[3] Department of Ophthalmology and Visual Sciences, University of Michigan, Ann Arbor, MI, USA
[4] Eye Center of Xiangya Hospital, Central South University, Changsha, Hunan Province, China
[5] Department of Ophthalmology, The First Affiliated Hospital of Nanjing Medical University, Nanjing, Jiangsu, China
[6] Institute for Bioengineering Research and Department of Mechanical Engineering, University of Kansas, Lawrence, KS, USA
[7] Hunan Key Laboratory of Ophthalmology, Changsha, Hunan Province, China

Correspondence: Yannis M. Paulus, W.K. Kellogg Eye Center, University of Michigan, 1000 Wall Street, Ann Arbor, MI 48105, USA. e-mail: ypaulus@med.umich.edu
Xinmai Yang, Institute for Bioengineering Research, University of Kansas, 3138 Learned Hall, 1530 W. 15th Street, KS 66045, USA. e-mail: xmyang@ku.edu
Xueding Wang, Department of Biomedical Engineering, University of Michigan, 2200 Bonisteel Boulevard, MI 48109, USA. e-mail: xdwang@umich.edu

Received: July 7, 2020
Accepted: September 24, 2020
Published: December 9, 2020

Keywords: photo-mediated ultrasound therapy; PUT; corneal neovascularization; angiogenesis; laser, ultrasound

Citation: Qin Y, Yu Y, Fu J, Xie X, Wang T, Woodward MA, Paulus YM, Yang X, Wang X. Photo-mediated ultrasound therapy for the treatment of corneal neovascularization in rabbit eyes. Trans Vis Sci Tech. 2020;9(13):16, https://doi.org/10.1167/tvst.9.13.16

Purpose: Corneal neovascularization (CNV) is the invasion of new blood vessels into the avascular cornea, leading to reduced corneal transparency and visual acuity, impaired vision, and even blindness. Current treatment options for CNV are limited. We developed a novel treatment method, termed photo-mediated ultrasound therapy (PUT), that combines laser and ultrasound, and we tested its feasibility for treating CNV in a rabbit model.

Methods: A suture-induced CNV model was established in New Zealand White rabbits, which were randomly divided into two groups: PUT and control. For the PUT group, the applied light fluence at the corneal surface was estimated to be 27 mJ/cm^2 at 1064-nm wavelength with a pulse duration of 5 ns, and the ultrasound pressure applied on the cornea was 0.43 MPa at 0.5 MHz. The control group received no treatment. Red-free photography and fluorescein angiography were utilized to evaluate the efficiency of PUT. Safety was evaluated by histology and immunohistochemistry. For comparison with the PUT safety results, conventional laser photocoagulation (LP) treatment was performed with standard clinical parameters: 532-nm continuous-wave (CW) laser with 0.1-second pulse duration, 450-mW power, and 75-µm spot size.

Results: In the PUT group, only 1.8% $\pm$ 0.8% of the CNV remained 30 days after treatment. In contrast, 71.4% $\pm$ 7.2% of the CNV remained in the control group after 30 days. Safety evaluations showed that PUT did not cause any damage to the surrounding tissue.

Conclusions: These results demonstrate that PUT is capable of removing CNV safely and effectively in this rabbit model.

Translational Relevance: PUT can remove CNV safely and effectively.

Introduction

Corneal neovascularization (CNV) is the invasion of new blood vessels into the avascular cornea, leading to reduced visual acuity. Pathologic CNV accounts for blindness in approximately 7 million people worldwide[1,2] and is a potential consequence of various disorders such as dry eye syndrome, contact lens use, corneal infections, surgery, trauma, and limbal stem cell deficiency.[3–5] Vascular ingrowth into the cornea is also a major risk factor for rejection after penetrating keratoplasty.[6] Therefore, treatment of CNV must be considered for visually impactful CNV or before keratoplasty procedures.[7]

Currently, anti-inflammatory and anti-vascular endothelial growth factor medications are the mainstay therapies for treating significant CNV.[7] However, none of these pharmacological treatments can permanently cure CNV, and they also have many side-effects, including glaucoma and infection.[8,9] Laser-based therapies for ablation of vessels are non-pharmacological therapies that have been used to target CNV.[10] Experimental and clinical studies have reported the use of laser thermal cauterization utilizing Nd:YAG lasers to remove CNV. In a recent investigation, a frequency-doubled Nd:YAG laser (532 nm) was used to treat 40 eyes in 40 patients with CNV. Successful occlusion of CNV occurred in only 53% of patients after 3 months. Complications included corneal hemorrhage, corneal thinning, vascularization exacerbation, and vessel lumen reopening.[11] Photodynamic therapy (PDT) is another approach for the occlusion of CNV[12]; however, a case series[13] showed evidence of vascular thrombosis and decreased CNV in only two-thirds of eyes that underwent PDT. PDT also has limited clinical utility due to its requiring a time-sensitive photosensitizer infusion, which can be disruptive and challenging in a busy clinic. In addition, PDT generates reactive oxygen species and requires the systemic injection of a photosensitizer, making the skin and eyes sensitive to light after the treatment and requiring patients to avoid sun exposure for several days. Furthermore, PDT may cause a photosensitivity reaction, dye extravasation, transient visual disturbances, infusion-related back pain, and even choroidal infarction, resulting in severe vision loss.

We have developed a novel, non-invasive, agent-free, and highly selective treatment by applying synchronized relatively low-intensity ultrasound bursts and nanosecond-duration laser pulses, referred to as photo-mediated ultrasound therapy (PUT).[14–19] The underlying mechanism of PUT is to promote cavitation activity precisely in the targeted microvessels by synchronizing the laser pulse to the rarefactional peak pressure of the ultrasound burst (i.e., in-phase setting).[20] The physiological functions of red blood cells, endothelial cells, and platelets can be directly impacted by the mechanical force induced by oscillating cavitation bubbles in the microvessels, resulting in vasocontraction, blood clot formation, and hemorrhage.[21–28]

In our previous studies, PUT was successfully used to remove the blood vessels in the choroid of rabbit eyes safely and effectively.[18] In this study, we established a system based on PUT technology for the treatment of CNV. The potential utilization of PUT in CNV treatment was tested via experiments in the suture-induced CNV model in the rabbit eye, and the outcomes were evaluated by comparing the treatment results for the PUT group with those of the control group. Safety results were compared with treatment by laser photocoagulation (LP), a laser technique that is used clinically to treat CNV.

Methods

PUT System

The schematic of the PUT system, which integrates a laser system with an ultrasound system, is shown in Figure 1. A standard Nd:YAG laser (Powerlite DLS 8010; Continuum, Santa Clara, CA) was used to provide 1064-nm light at a pulse repetition rate of 10 Hz and pulse width of 5 ns. The main laser beam was directed by dichroic mirrors to the focal spot of a high-intensity focused ultrasound (HIFU) transducer (H-107, center frequency 0.5 MHz; Sonic Concepts, Bothell, WA), which has a geometric focal distance of 62.6 mm, a focal depth of 21.42 mm, and a focal width of 3.02 mm. The applied laser intensity was carefully adjusted by controlling the Q-switch delay time. The laser spot was adjusted to 3 mm in diameter on the cornea by controlling the size of the pinhole. An optical power meter was used to measure the laser pulse energy in real time through the light reflected from a dichroic mirror. The ultrasound system included a function generator (DS345; Stanford Research System, Sunnyvale, CA), which produced 0.5-MHz bursts (10 ms long) at a repetition rate of 10 Hz; a radio frequency (RF) power amplifier (2100L; Eni Technology, Inc., Rochester, NY); and a HIFU transducer. The HIFU transducer was connected to the RF power amplifier through an H-107 impedance matching network. The focal pressure of the HIFU transducer was calibrated with a standard fiberoptic probe hydrophone (HNC-1500; Onda Corporation,

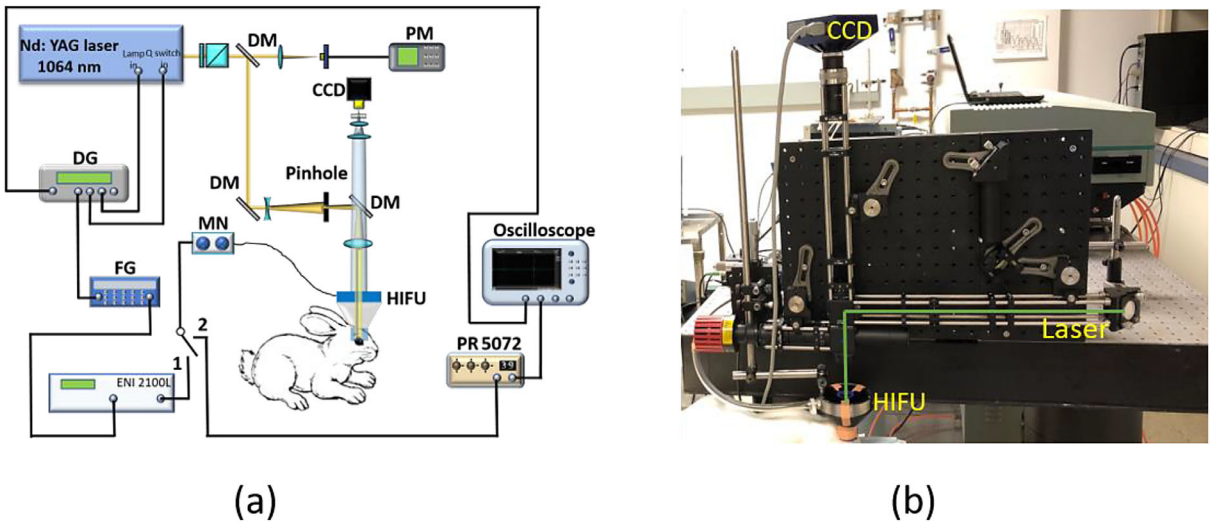

Figure 1. (a) Schematic of the experiment setup for rabbit CNV treatment in vivo. (b) Photograph of the PUT system. DM, dichroic mirrors; PM, power meter; DG, delay generator; FG, function generator; MN, matching network for HIFU transducer; PR, pulser/receiver.

Sunnyvale, CA). The duty cycle of HIFU bursts was set to 10% to avoid significant heat generation. A pulse delay generator (DG355; Stanford Research Systems, Inc., Sunnyvale, CA) with a precision within 1 ps was used to synchronize the laser and the ultrasound systems with the repetition rate of 10 Hz. A charge-coupled device (CCD) was applied to monitor the treatment effect in real time, and its illumination light was provided by three pico light-emitting diodes, which were integrated in the cover of the coupling cone.

Although light travels so fast that it can be considered instantaneous in the current study, ultrasound waves take longer time to travel from the transducer to the target. To synchronize the laser pulse to the rarefactional peak pressure of ultrasound at the target (i.e., in-phase setting), it was necessary to determine the time delay between the fire of each laser pulse and the fire of each ultrasound burst. This delay time can be calculated by measuring the time of flight for a photoacoustic (PA) pulse to travel from the target to the HIFU transducer in addition to the system delay time.[20] In the current setup, the PA pulse can be produced when the 1064-nm light illuminates the target. A pulser/receiver (5072PR; Olympus NDT, Inc., Waltham, MA) was used to receive and amplify the PA signal detected by the HIFU transducer when the switch (shown in Fig. 1a) was connected to position 2, and then the time of flight was measured by an oscilloscope (TDS540; Tektronix, Inc., Beaverton, OR). When the time delay between the fire of each laser pulse and the fire of each ultrasound burst had been calculated, by adjusting the time difference between the trigger for the laser system and the trigger for the ultrasound system each laser pulse and ultrasound burst was properly synchronized at the target for PUT, with the switch shown in Figure 1a connected to position 1.

Experimental Animal Care and Handling

New Zealand White rabbits (2.5–3.0 kg; 3–8 months old; both genders) were acquired by generous donation from the Center for Advanced Models for Translational Sciences and Therapeutics at the University of Michigan Medical School. The animals were housed in an air-conditioned room with a 12-hour light/dark cycle, fed standard laboratory food, and allowed free access to water. All of the animal handling procedures were carried out in compliance with protocols approved by the Institutional Animal Care and Use Committee at the University of Michigan (PRO00008567, PI YMP), with strict adherence to the ARVO Statement for the Use of Animals in Ophthalmic and Vision Research.

Induction of CNV Model

Twenty-one rabbits were used in this study. Each rabbit was anesthetized with a combination of 40 mg/kg ketamine hydrochloride (Ketalar; Par Pharmaceutical, Spring Valley, NY) and 5 mg/kg xylazine (Anased; MWI Veterinary Supply Co./VetOne, Boise, ID) injected intramuscularly, and topical anesthesia was also provided by applying proparacaine (Alcaine; Alcon, Fort Worth, TX). Only one eye of each rabbit was used. CNV was induced according to a previous method.[29] Briefly, a 7-0 silk suture was passed through the corneal stroma 1.5 mm

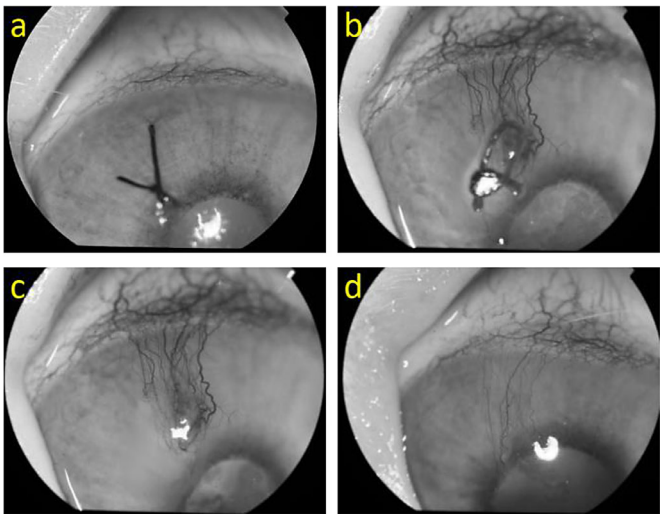

Figure 2. Red-free photographs of the rabbit cornea demonstrating development of the CNV model with a suture. (a) Immediately after suture placement. (b) Six weeks after suture placement, demonstrating the robust development of CNV. (c) Immediately after suture removal, 6 weeks after suture placement. (d) One week after suture removal, showing a reduction in CNV. The CNV at this time (1 week after suture removal) is stable.

away from the limbus and vertical to the limbus with a length of 3 mm to induce CNV. Six weeks after suture placement, sufficient stable corneal angiogenesis was observed, and the suture was removed. After removal of the suture, there was in the first week a mild regression in CNV that then stabilized by 1 week after suture removal, with the remaining CNV stably sustained for more than 1 month. Thus, 1 week after suture removal was selected as the time for PUT treatment. Figure 2 shows the red-free photographs of the cornea at different time points, including immediately after suture placement, 6 weeks after suture placement, immediately after suture removal, and 1 week after suture removal. All of the red-free photographs were taken using a clinical ophthalmic photography system (TRC 50EX; Topcon Corporation, Tokyo, Japan) in the anterior segment mode. We also performed fluorescein angiography to check the perfusion and leakage of the CNV. Because the cornea is an avascular and transparent tissue and the iris is full of blood vessels, the red-free photographs provided a higher contrast ratio than fluorescein angiography photographs. For this reason, we used the red-free photographs to quantify the CNV. The 21 rabbits were randomly assigned to three groups as follows: group 1, PUT treatment ($n = 9$); group 2, no treatment (controls, $n = 6$); and group 3, laser photocoagulation (LP) therapy treatment ($n = 6$). Animals were imaged at the following times: before treatment, immediately at the time of treatment, and 7, 14, 21, and 30 days after treatment.

Imaging Processing and Neovascular Quantification

Image processing was performed by using red-free photographs to quantify the CNV changes in the target area. First, we manually selected the treatment area on each red-free photograph by using Photoshop (Adobe, Mountainview, CA). Second, the adaptive histogram equalization function in MATLAB (MathWorks, Natick, MA) was used to enhance the contrast between the CNV and the surrounding tissue. The CNV path was then segmented using the edge detection method in MATLAB. When we had identified the CNV path, the pixels of the CNV in the treated region in the post-processing red-free photographs were counted. In each sample, to get the relative neovascular density percentage, the pixel numbers were normalized by the number of pixels before treatment (*Prior*), as shown in the following equation:

$$Relative\ neovascular\ density\ percentage = \frac{CNV\ pixel\ numbers\ (each\ time\ point)}{CNV\ pixel\ numbers\ (Prior)} \times 100\%$$

Safety Evaluation

Histological Analysis of Cornea and Limbus

One week, 1 month, and 3 months after treatment, one rabbit from the PUT group and one rabbit from the control group, along with one rabbit from the LP group, were euthanized. The eye was immediately enucleated and fixed in 10% formalin solution for 48 hours and then preserved in 70% ethanol until processing. The corneal and limbal CNV area of each eye was removed and sectioned into two to four strips of approximately equal width (3–4 mm) before being embedded into paraffin blocks. The paraffin-embedded sections containing tissue of the corneal and limbal CNV area (thickness 5 µm) were processed with a microtome and stained with hematoxylin and eosin (H&E). A part of the limbal tissue was subjected to immunohistochemical staining with anti-p63 antibody (1:400; Invitrogen, Carlsbad, CA). These sections were analyzed under a light microscope (BX51; Olympus Corporation, Tokyo, Japan). Photographs were taken with an Olympus DP70 digital camera.

The thicknesses of the cornea and corneal epithelium were analyzed by ImageJ software (version 1.51j8; National Institutes of Health, Bethesda, MD). Five different areas of the cornea and corneal epithelium were measured to obtain an average value of the thickness.

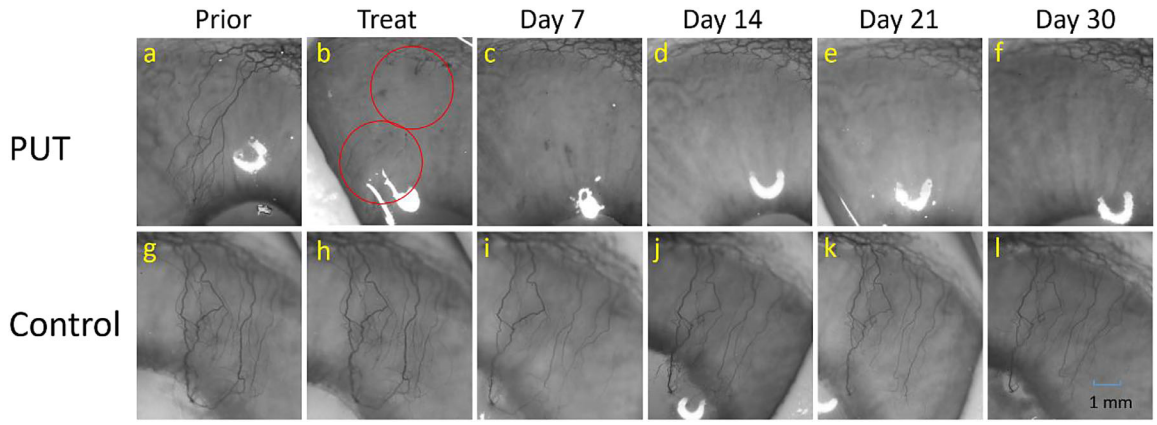

Figure 3. Red-free photographs of rabbit CNV before and after PUT treatment in comparison with results from the control group at the same time points. (a–f) Red-free photographs of one case in the PUT treatment group. The *red circles*, which have a diameter of 3 mm, indicate the treatment areas (b). The applied ultrasound pressure was 0.43 MPa at 0.5 MHz, the applied laser fluence was 27 mJ/cm^2 at 1064 nm, and the treatment duration in each *red circle* was 10 minutes. (g–l) Red-free photographs of one case in the control group. Prior, 1 day before the treatment (1 week after suture removal); Treat, immediately after treatment.

For semiquantitative evaluation of immunohistochemistry in the limbus, for each group one representative high-power field (HPF) at 40× magnification was used. A scoring system ranging from 0 to 4 was applied to represent all positively stained cells per HPF on a percentage basis: 0% (score 0), 1% to 33% (score 1), 34% to 67% (score 2), 68% to 99% (score 3), and 100% (score 4).[30]

Corneal Endothelium Staining and Evaluation of Endothelial Density

One rabbit from each of the PUT treatment, LP treatment, and control groups was euthanized at each time point of 1 week, 1 month, and 3 months after treatment.

The treated eye was enucleated, and the entire cornea was then dissected and positioned endothelial side up. Alizarin red 0.2% (pH 4.2; Sigma-Aldrich, St. Louis, MO) was applied to the cornea dropwise for 3 minutes. The cornea was then washed with phosphate-buffered saline (PBS), and 0.25% Trypan Blue solution (Sigma-Aldrich) was applied dropwise for 90 seconds followed by another wash with PBS. After a final rinse with PBS, the cornea was cut into four pieces, and each piece of the cornea was placed with the endothelial side down on a coverslip. The mounted slide was first examined under an Olympus BX51 light microscope with 100× low power field (10× objective lens). After localization, cells were then analyzed with 400× final magnification (40× objective). Photographs were taken with an Olympus DP70 digital camera. At least 10 HPFs were examined for endothelial cells. The number of endothelial cells per HPF was marked and counted. The endothelial density was analyzed using Imaris 9.1.0 imaging analysis software (Bitplane AG, Zürich, Switzerland).

Statistical Analysis

Differences in the thickness of cornea, thickness of corneal epithelium, and density of corneal endothelium in three post-treatment groups (1 week, 1 month, and 3 months) were compared to before-treatment groups independently using *t*-tests with SPSS Statistics (IBM, Armonk, NY). Differences in the three post-treatment groups (1 week, 1 month, and 3 months) were compared to before-treatment groups independently with semiquantitative evaluation of the immunohistochemistry of the limbus using Mann–Whitney U tests. Benjamini–Hochberg correction was performed on all statistical analyses. The false discovery rate was 0.05.

Results

Efficiency of PUT Treatment Compared to Control

In the PUT treatment group, nine rabbits in total were treated with 0.43-MPa ultrasound pressure at 0.5 MHz and 27 mJ/cm^2 laser fluence at 1064 nm. One sample case from the PUT treatment group is shown in Figures 3a to 3f. In Figure 3b, the red circles, 3 mm in diameter, indicate the treatment areas. Immediately (less than 1 minute) after PUT treatment, most of the CNVs in the treatment areas were removed, with slight hemorrhage noticed, as shown in Figure 3b. At 7 days after PUT treatment, 92.4%

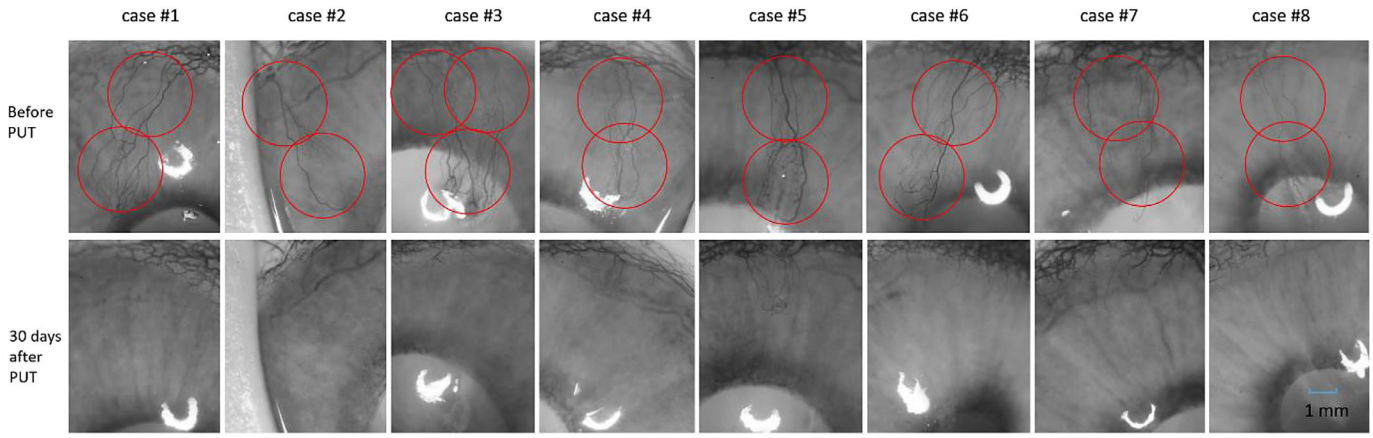

Figure 4. Red-free photographs of rabbit CNV before and at 30 days after PUT treatment (eight cases). The *red circles* show the treatment areas, which have a diameter of 3 mm. A significant reduction in CNV at 30 days after PUT treatment can be observed. The applied ultrasound pressure was 0.43 MPa at 0.5 MHz, the applied laser fluence was 27 mJ/cm^2 at 1064 nm, and the treatment duration in each treatment area was 10 minutes.

of the CNV has disappeared, and it persisted to 30 days after PUT treatment, which was the longest observation time in this study. All eight cases in the PUT treatment group were observed up to 30 days as shown in Figure 4. By comparing the red-free photographs acquired before and at 30 days after the PUT treatment, the efficiency of PUT in removing CNV was demonstrated.

In the control group, five rabbits were observed at the same time points as the PUT treatment group. One sample control case is shown in Figures 3m to 3r. We observed that the CNV was stable up to 30 days. All five rabbits, which were observed up to 30 days, had similar results, as shown in Figure 5.

Figure 6 shows the normalized relative CNV intensities of the PUT treatment and control groups before the treatment (Prior) and at 7, 14, 21, and 30 days after treatment. In the control group, the results indicate that the CNV was stable during the 30 days of observation with a slight decline in CNV density; 71.4% ± 7.2% of the CNV remained at day 30. In the PUT treatment group, there was a very rapid decline in CNV by 7 days after treatment that persisted over time, resulting in only 1.8% ± 0.8% neovascularization remaining at 30 days after treatment. The quantification results further demonstrated that PUT holds great promise for CNV treatment.

Safety Evaluation

The findings from the safety evaluation for PUT treatment and LP treatment are shown in Figure 7. Changes in the corneal stroma were evaluated by H&E histology. At the time when the suture was removed, the cornea showed obvious inflammation and neovascularization, as shown in Figure 7b. In the PUT treatment group, the corneal stroma returned to normal by 1 week after treatment and remained normal for 3 months. The corneal fibrils and collagen were well organized after the treatment. No neovascularization or inflammatory cells were observed in the stroma, as shown in Figures 7c, 7e, and 7g. In the LP treatment group, there were circular stromal scars that persisted for more than 3 months, as shown in Figures 7d, 7f, and 7h. Polymorphonuclear leukocytes, inflammatory debris, and neovascularization filled clefts between the stromal lamellae, although they were significantly reduced compared to before treatment (Fig. 7b).

The thickness of corneal epithelium was measured before PUT or LP treatment and at different time points after each treatment. In the suture-removal model, the thickness of corneal epithelium showed no statistical difference from the normal cornea (i.e., comparing "before" and "normal in Fig. 7i). At 1 week after PUT treatment, the corneal epithelium was thinner than before ($P < 0.05$), but the corneal epithelium proliferated and recovered rapidly during the next 3 months of observation, as shown in Figure 7i. After LP treatment, the corneal epithelium was also thinner at 1 week after treatment, and the recovery of the corneal epithelium during the next 3 months was not as rapid as for the PUT treatment group.

The thickness of the cornea was measured before PUT or LP treatment and at different time points after each treatment. Compared with the thickness of normal cornea, the cornea at the time of suture removal

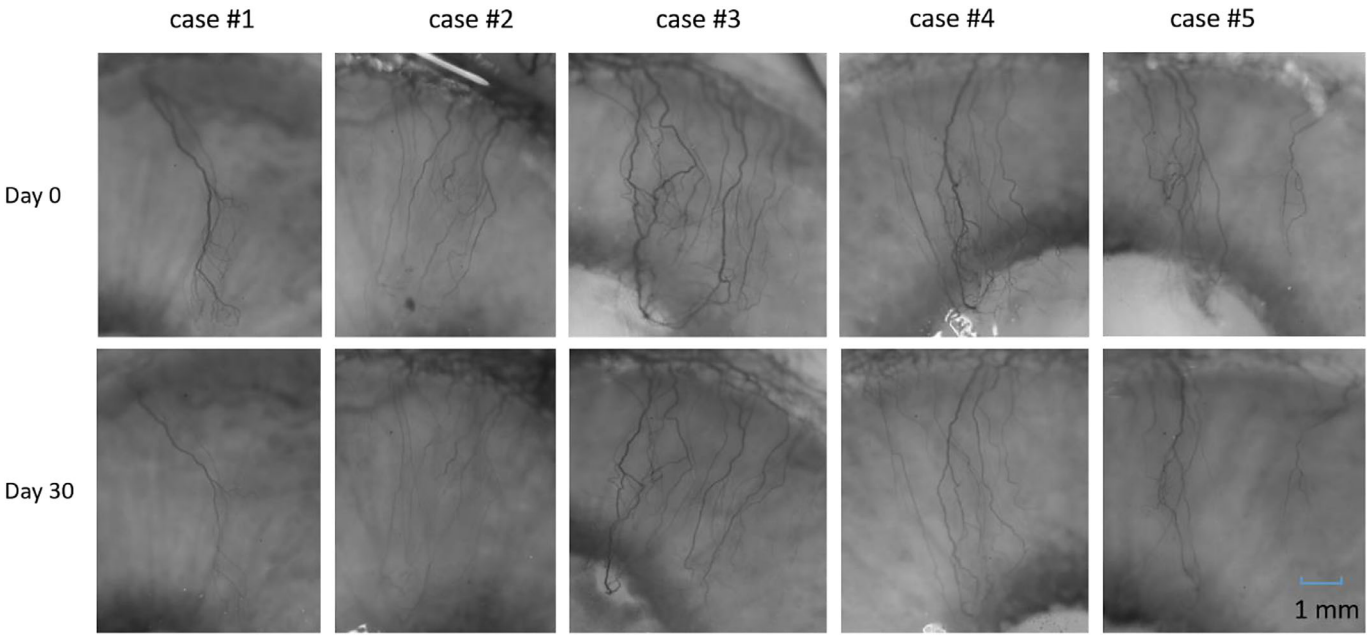

Figure 5. Red-free photographs of rabbit corneal neovascularization at day 0 and day 30 in the control group (five cases). They clearly show that the CNV in this model persisted for 30 days in the control eyes, with a slight decline in CNV density.

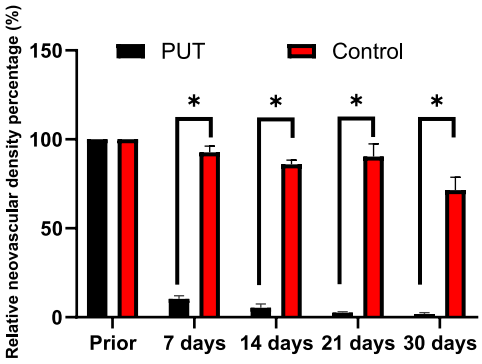

Figure 6. Statistical analysis of the normalized neovascularization density of the PUT treatment group ($n = 8$) and the control group ($n = 5$) at different time points after treatment. *Statistically significant difference.

was thicker with a corneal inflammatory response. After LP treatment, the thickness of the cornea was thinner at both 1 week and 1 month after treatment but was recovered by 3 months after treatment. A similar corneal thinning effect after LP treatment has been reported in other studies, with some studies even reporting resulting corneal ectasia resulting in keratoconus.[7,11,31,32] In our study, after PUT treatment, there was no obvious change in the thickness of the cornea.

The characteristics of the limbus and the analysis of cell marker p63 after PUT or LP treatment are shown in Figure 8. The limbal epithelium thickness of the suture-removal model was not affected compared to the normal group, but the frequency and expression of limbal stem cell marker p63 were higher in the suture-removal group. One week after PUT treatment, the limbal epithelium was thicker and the percentage of expression of p63 was a little higher, but without statistical difference, possibly due to the limbus being needed to proliferate new epithelium to cover the cornea after the corneal epithelium was damaged after PUT. At 1 and 3 months after PUT treatment, the limbal thickness was back to normal, and the percentage of the limbal stem cells showed no difference from normal, suggesting that PUT treatment did not affect the function of limbal stem cells. In the LP treatment group, the limbal epithelium was thinner after the treatment and did not return to normal for at least 3 months. The number of limbal stem cells also decreased after treatment, and the decreased level persisted for at least 3 months. By comparing these two groups, we concluded that PUT treatment did not affect the number or the function of the limbal stem cells, which is not the case for LP treatment.

Endothelial staining results and quantitative analysis for different treatment groups (i.e., PUT and LP) at different time points are shown in Figure 9. There was

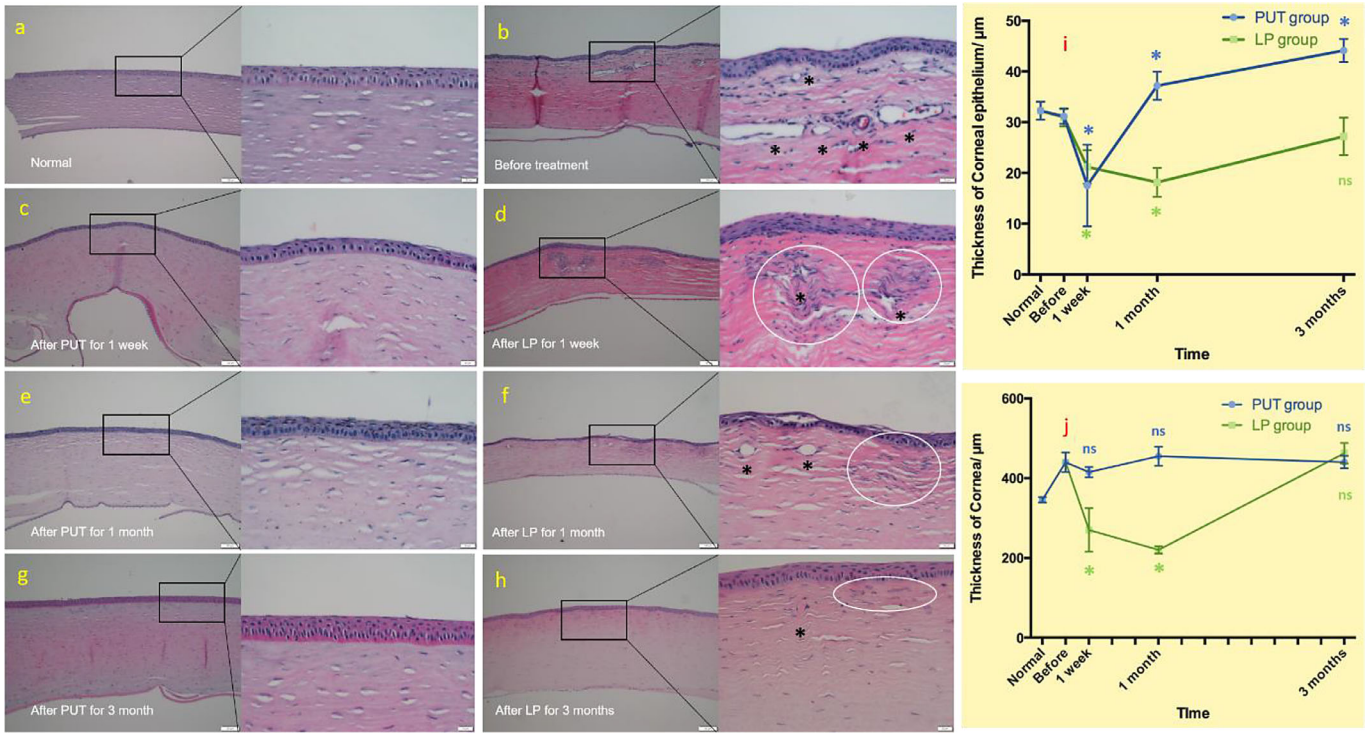

Figure 7. Structural characteristics of the cornea. H&E staining of normal cornea (a), suture-removal cornea (b), and cornea after PUT treatment for 1 week (c), 1 month (e), and 3 months (g). H&E staining of cornea after LP treatment for 1 week (d), 1 month (f), and 3 months (h). *White circles* indicate fibrosis and inflammatory cells. *Black asterisks* indicate neovascularization. Changes of the thickness of corneal epithelium (i) and total cornea (j) in the two different treatment groups (PUT and LP) are compared. For the thickness of the corneal epithelium compared to the before-treatment result, *P* values for the PUT group were 0.0161, 0.0207, and 0.0001 for 1 week, 1 month, and 3 months, respectively; *P* values for the LP group were 0.0052, 0.0013, and 0.1542 for 1 week, 1 month, and 3 months, respectively. For the thickness of the cornea compared to the before-treatment result, *P* values for the PUT group were 0.1381, 0.4985, and 0.9722 for 1 week, 1 month, and 3 months, respectively; *P* values for the LP group were 0.0014, 0.00002, and 0.5472 for 1 week, 1 month, and 3 months, respectively. The error bars show the mean and SD for measurements at different locations of cornea. The *green asterisks* indicate a statistically significant difference compared to the before-treatment result; ns, no statistically significant difference.

no statistical difference at the time of suture removal when compared to normal. After PUT or LP treatment, the density of the endothelium was not affected in either group, as shown in Figure 9i.

Discussion

To our knowledge, this study demonstrates for the first time the feasibility of PUT to treat CNV. The treatment results from the rabbit CNV model demonstrated that after one-time PUT treatment, only 1.8% ± 0.8% neovascularization remained at 30 days post-treatment, indicating that PUT is a safe and efficient method for removing CNV.

The safety of PUT was evaluated against LP therapy. The mechanism of LP therapy to treat neovascularization is based on a laser thermal effect to coagulate vessels. As demonstrated by our experiments, complications of LP therapy on the cornea include corneal thinning, corneal and limbal epithelium thinning, vessel lumen reopening, corneal stromal fibrosis, and limbal stem cell damage. As a member of the p53 tumor suppressor gene family, transcription factor p63 is an essential parameter in the development of a stratified epithelium and is also associated with the proliferative capacity.[30] The percentage of cells expressing p63 was decreased in the LP group, indicating limbal stem cell damage. These side-effects have also been reported by other studies involving LP treatment on the cornea.[7,11,31,32] PUT removes neovascularization through a completely different mechanism, which is to directly damage vascular endothelial cells through the mechanical forces produced via cavitation.[14–18] The safety evaluation results demonstrated that either corneal thickness, limbal epithelium, limbal stem cell, and corneal stroma were not affected by PUT treatment or the effect is reversible. The corneal epithelium was thinner at 1 week after PUT but rapidly proliferated

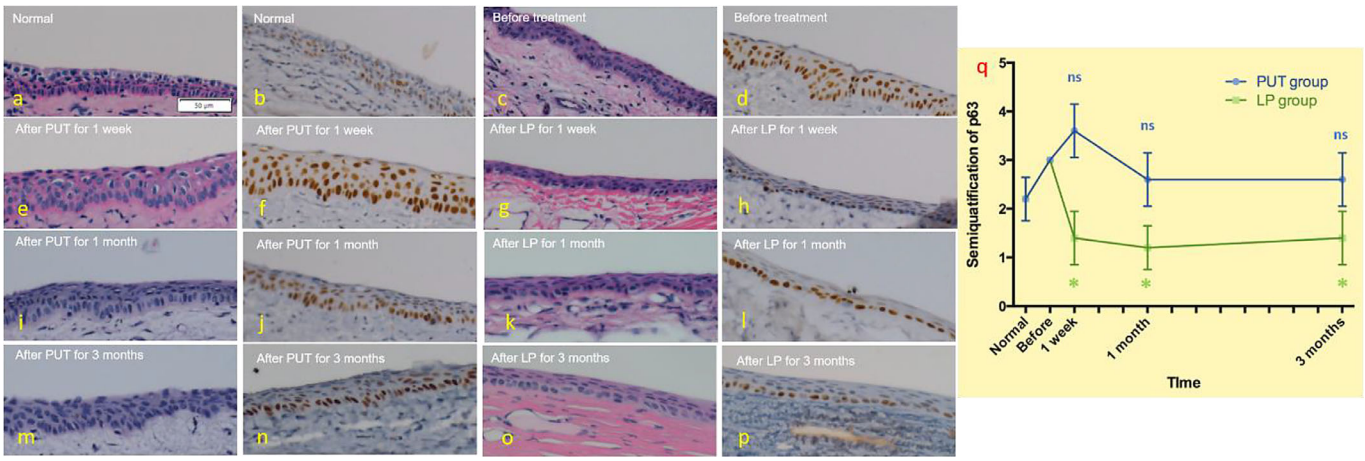

Figure 8. Structural characteristics of the limbus. H&E staining and immunohistochemistry staining of limbal stem cell marker p63 on the limbus (a–p). Representative pictures of the limbus in PUT and LP treatment groups at different time points. Limbal stem cell marker p63 was present in every examined region with increasing frequency in the PUT treatment group after 1 week and returned to normal at 1 and 3 months. In the LP treatment group, p63 demonstrated a decrease at 1 week that persisted for at least 3 months. (q) Semiquantitative analysis of immunohistochemical staining for proliferation, differentiation, and stem cell markers; the error bars show the mean and SD for measurements at different locations of limbal epithelium. In the PUT treatment group, p63 showed a temporary increase after suture removal and at 1 week after treatment (without a statistically significant difference) and then decreased to normal at 1 and 3 months after treatment. In the LP treatment group, p63 decreased at 1 week after treatment, and the decrease persisted for at least 3 months. For the semiquantitative analysis of immunohistochemical staining of p63, compared to the before-treatment result, *P* values for the PUT group were 0.0334, 0.911, and 0.911 for 1 week, 1 month, and 3 months, respectively; *P* values for the LP group were 0.02791, 0.01046, and 0.02791 for 1 week, 1 month, and 3 months, respectively. The *green asterisks* indicate a statistically significant difference compared to the before-treatment result; ns, no statistically significant difference.

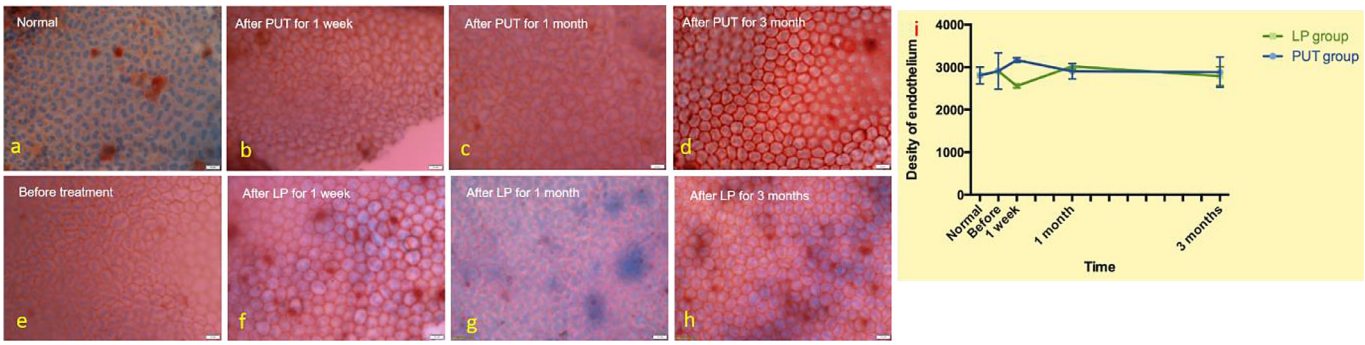

Figure 9. Endothelial staining of PUT (a–d) and LP (e–f) treatment groups at different time points. (i) Quantification of endothelial density for the different groups at different time points demonstrated no difference in the density of corneal endothelial cells. For endothelial density, compared to the before-treatment result, *P* values for the PUT group were 0.6991, 0.4041, and 0.9918 for 1 week, 1 month, and 3 months, respectively; *P* values for the LP group were 0.311, 0.4482, and 0.9927 for 1 week, 1 month, and 3 months, respectively.

and became thicker (hyperplastic), a condition referred to as pseudoepitheliomatous hyperplasia,[33] which is a benign proliferation of the conjunctival or corneal epithelium that occurs in response to inflammatory conditions. Sometimes it occurs after laser treatment.[34] According to the safety evaluation results from the two treatment groups (PUT and LP), we can conclude that PUT may transiently change the ocular surface, but the corneal function is not damaged.

By taking advantage of the high intrinsic optical contrast between hemoglobin and other tissues, PUT, via the synergy of safe laser pulses and ultrasound bursts, induces cavitation that occurs only in the target blood vessels. Hence, the treatment effect in PUT is precisely localized in blood vessels only, and unwanted collateral damage to the surrounding tissue can be largely avoided. Offering this unique advantage, PUT may improve the clinical management of eye diseases,

including treatment of CNV, by delivering selective treatment of pathologic vessels with minimized side effects and improved patient outcomes. In the future, PUT can also possibly be used to treat choroidal or retinal neovascularization. Because PUT removed CNV safely and effectively in the rabbit disease model and our current PUT system is designed for large eyes such as human or rabbit eyes, PUT can be translated to human trials in the future.

Acknowledgments

The authors thank Yuqing Chen, and the Center for Advanced Models and Translational Sciences and Therapeutics at the University of Michigan Medical School for the generous donation of the rabbits used in this study. We also thank David Musch, PhD, for providing his statistical expertise and recommendation.

Supported in part by grants from the National Eye Institute, National Institutes of Health (1R01EY029489, XY; 1K08EY027458, YMP; 1R01EY031033, MAW), by the Alliance for Vision Research (YMP), and by unrestricted departmental support from Research to Prevent Blindness (YMP). This work utilized the Vision Research Core Center funded by the National Eye Institute (P30EY007003).

Disclosure: **Y. Qin,** None; **Y. Yu,** None; **J. Fu,** None; **X. Xie,** None; **T. Wang,** None; **M.A. Woodward,** None; **Y.M. Paulus,** University of Michigan and University of Kansas (P), PHOTOSONOX LLC (F); **X. Yang,** University of Michigan and University of Kansas (P), PHOTOSONOX LLC (F); **X. Wang,** University of Michigan and University of Kansas (P), PHOTOSONOX LLC (F)

* YQ and YY contributed equally to this article.

References

1. Kim RY, Chung SK, Kim MS, Ra H. Effects of combined photodynamic therapy and topical bevacizumab treatment on corneal neovascularization in rabbits. *Cornea*. 2016;35(12):1615–1620.
2. Shahsuvaryan ML. Therapeutic potential of ranibizumab in corneal neovascularization. *Trends Pharmacol Sci*. 2017;38(8):667–668.
3. Hamill CE, Bozorg S, Chang H-YP, et al. Corneal alkali burns: a review of the literature and proposed protocol for evaluation and treatment. *Int Ophthalmol Clin*. 2013;53(4):185–194.
4. Lee P, Wang CC, Adamis AP. Ocular neovascularization: an epidemiologic review. *Surv Ophthalmol*. 1998;43(3):245–269.
5. Lim P, Fuchsluger TA, Jurkunas UV. Limbal stem cell deficiency and corneal neovascularization. Semin *O*phthalmol. 2009;24(3):139–148.
6. Bachmann B, Taylor RS, Cursiefen C. Corneal neovascularization as a risk factor for graft failure and rejection after keratoplasty: an evidence-based meta-analysis. *Ophthalmology*. 2010;117(7):1300–1305.e7.
7. Roshandel D, Eslani M, Baradaran-Rafii A, et al. Current and emerging therapies for corneal neovascularization. *Ocul Surf*. 2018;16(4):398–414.
8. Sulaiman RS, Kadmiel M, Cidlowski JA. Glucocorticoid receptor signaling in the eye. *Steroids*. 2018;133:60–66.
9. Pan Q, Xu Q, Boylan NJ, et al. Corticosteroid-loaded biodegradable nanoparticles for prevention of corneal allograft rejection in rats. *J Control Release*. 2015;201:32–40.
10. Baradaran-Rafii A, Delfazayebaher S, Aghdami N, Taghiabadi E, Bamdad S, Roshandel D. Midterm outcomes of penetrating keratoplasty after cultivated oral mucosal epithelial transplantation in chemical burn. *Ocul Surf*. 2017;15(4):789–794.
11. Kumar J, Gehra A, Sirohi N. Role of frequency doubled Nd:Yag laser in treatment of corneal neovascularisation. *J Clin Diagn Res*. 2016;10(4):NC01–NC04.
12. Al-Abdullah AA, Al-Assiri A. Resolution of bilateral corneal neovascularization and lipid keratopathy after photodynamic therapy with verteporfin. *Optometry*. 2011;82(4):212–214.
13. Al-Torbak AA. Photodynamic therapy with verteporfin for corneal neovascularization. *Middle East Afr J Ophthalmol*. 2012;19(2):185–189.
14. Hu Z, Zhang H, Mordovanakis A, et al. High-precision, non-invasive anti-microvascular approach via concurrent ultrasound and laser irradiation. *Sci Rep*. 2017;7:40243.
15. Li S, Qin Y, Wang X, Yang X. Bubble growth in cylindrically-shaped optical absorbers during photo-mediated ultrasound therapy. *Phys Med Biol*. 2018;63(12):125017.
16. Yang X, Hu Z, Zhang H, Mordovanakis A, Paulus YM, Wang X. Antivascular photo-mediated ultrasound therapy. In: *2016 IEEE International Ultrasonics Symposium (IUS)*. Piscataway, NJ: Institute of Electrical and Electronics Engineers; 2016:1–4.

17. Yang X, Zhang H, Li J, Paulus Y, Wang X. The application of antivascular photo-mediated ultrasound therapy in removing microvessels in the eye. In: *2017 IEEE International Ultrasonics Symposium (IUS)*. Piscataway, NJ: Institute of Electrical and Electronics Engineers; 2017: 1–1.
18. Zhang H, Xie X, Li J, et al. Removal of choroidal vasculature using concurrently applied ultrasound bursts and nanosecond laser pulses. *Sci Rep*. 2018;8(1):12848.
19. Zhang W, Qin Y, Xie X, et al. Real-time photoacoustic sensing for photo-mediated ultrasound therapy. *Opt Lett*. 2019;44(16):4063–4066.
20. Qin Y, Yu Y, Xie X, et al. The effect of laser and ultrasound synchronization in photo-mediated ultrasound therapy. *IEEE Trans Biomed Eng*. 2020;67(12):3363–3370.
21. Ballermann BJ, Dardik A, Eng E, Liu A. Shear stress and the endothelium. *Kidney Int Suppl*. 1998;67:S100–S108.
22. Hwang JH, Brayman AA, Reidy MA, Matula TJ, Kimmey MB, Crum LA. Vascular effects induced by combined 1-MHz ultrasound and microbubble contrast agent treatments in vivo. *Ultrasound Med Biol*. 2005;31(4):553–564.
23. Li Y-SJ, Haga JH, Chien S. Molecular basis of the effects of shear stress on vascular endothelial cells. *J Biomech*. 2005;38(10):1949–1971.
24. Wood AK, Ansaloni S, Ziemer LS, Lee WM-F, Feldman MD, Sehgal CM. The antivascular action of physiotherapy ultrasound on murine tumors. *Ultrasound Med Biol*. 2005;31(10):1403–1410.
25. Wood AK, Bunte RM, Cohen JD, Tsai JH, Lee WM-F, Sehgal CM. The antivascular action of physiotherapy ultrasound on a murine tumor: role of a microbubble contrast agent. *Ultrasound Med Biol*. 2007;33(12):1901–1910.
26. Mukundakrishnan K, Ayyaswamy P, Eckmann D. Bubble motion in a blood vessel: shear stress induced endothelial cell injury. *J Biomech Eng*. 2009;131(7):074516.
27. Hu X, Kheirolomoom A, Mahakian LM, et al. Insonation of targeted microbubbles produces regions of reduced blood flow within tumor vasculature. *Invest Radiol*. 2012;47(7):398–405.
28. Feng G, Liu J, Zhao X, et al. Hemostatic effects of microbubble-enhanced low-intensity ultrasound in a liver avulsion injury model. *PLoS One*. 2014;9(5):e95589.
29. Énzsöly A, Markó K, Tábi T, et al. Lack of association between VAP-1/SSAO activity and corneal neovascularization in a rabbit model. *J Neural Transm*. 2013;120(6):969–975.
30. Kammergruber E, Rahn C, Nell B, Gabner S, Egerbacher M. Morphological and immunohistochemical characteristics of the equine corneal epithelium. *Vet Ophthalmol*. 2019;22(6):778–790.
31. Parsa CF, Temprano J, Wilson D, Green WR. Hemorrhage complicating YAG laser feeder vessel coagulation of cornea vascularization. *Cornea*. 1994;13(3):264–268.
32. Marsh RJ. Argon laser treatment of lipid keratopathy. *Br J Ophthalmol*. 1988;72(12):900–904.
33. Seoane J, González-Mosquera A, García-Martín J-M, García-Caballero L, Seoane-Romero J-M, Varela-Centelles P. Pseudoepitheliomatous hyperplasia after diode laser oral surgery. An experimental study. *Med Oral Patol Oral Cir Bucal*. 2015;20(5):e554–e559.
34. Reddy SV, Husain D. Panretinal photocoagulation: a review of complications. Semin Ophthalmol. 2018:33(1):83–88.